

The dynamic bulk modulus of three glass-forming liquids

Ditte Gundermann, Kristine Niss, Tage Christensen, Jeppe C. Dyre, and Tina Hecksher
 DNRF Centre Glass and Time, IMFUFA, Department of Sciences, Roskilde University, Postbox 260,
 DK-4000 Roskilde, Denmark

(Received 4 March 2014; accepted 4 June 2014; published online 26 June 2014)

We present dynamic adiabatic bulk modulus data for three organic glass-forming liquids: two van der Waal's liquids, trimethyl-pentaphenyl-trisiloxane (DC705) and dibutyl phthalate (DBP), and one hydrogen-bonded liquid, 1,2-propanediol (PD). All three liquids are found to obey time-temperature superposition within the uncertainty of the measurement in the adiabatic bulk modulus. The bulk modulus spectra are compared to the shear modulus spectra. The time scales of the two responses were found to be similar. The shapes of the shear and bulk modulus alpha loss peak are nearly identical for DBP and DC705, while the bulk modulus spectrum for PD is significantly broader than that of the shear modulus. The data further suggest that a "bulk modulus version of the shoving model" for the temperature dependence of the activation energy using the bulk modulus relaxation strength, $\Delta K(T)$, works well for DC705 and DBP, but not PD, while a formulation of the model using the high-frequency plateau value, $K_\infty(T)$, gave a poor result for all three liquids. © 2014 AIP Publishing LLC. [<http://dx.doi.org/10.1063/1.4883736>]

I. INTRODUCTION

As liquids are cooled below the melting point without crystallizing, the viscosity increases enormously.¹⁻³ This has the effect that all thermal, mechanical, electrical, etc., response functions become time or, equivalently, frequency dependent on a time scale of seconds to hours, even days or weeks,^{4,5} i.e., the liquids display both liquid and solid behavior, depending on the time scale of observation.

Understanding the microscopic dynamics leading to the observed macroscopic behavior of supercooled liquids is the goal of the study of viscous liquid dynamics and glass formation. Direct access to the dynamics on a microscopic level is however difficult at best; experimentally accessible quantities are mostly macroscopic. But different macroscopic response functions probe the underlying microscopic dynamics in different ways, and thus understanding the relation between the different response functions is an important step towards understanding the nature of viscous liquids.

The bulk modulus is the pressure response to a shape preserving volume deformation, defined as $K = -V \frac{\delta p}{\delta V}$. Such a response can be measured under two different conditions, namely, adiabatic (K_S) or isothermal (K_T). Whether the isothermal or the adiabatic bulk modulus is measured depends on the geometry and size of the measuring cell and the frequency range explored.

Data on the *dynamic* bulk modulus are scarce in literature, because measuring this quantity is a notoriously difficult task and few techniques exist that meet the challenge. In the literature, studies exist, e.g., Refs. 6-9, that report bulk moduli determined indirectly from a measured set of other elastic moduli, thus utilizing the fact that for isotropic solids there are only two independent elastic constants.¹⁰ But one has to be very cautious when doing so and make sure that the two moduli are measured under identical experimental conditions. Otherwise, there is the risk that spurious effects due to,

e.g., difference in temperature calibration, dominate the results. This issue is discussed by Tschoegl and Knauss¹¹ and we return to this topic below in Sec. III B.

To the best of our knowledge, only three fundamentally different techniques that give a direct measure of the dynamic bulk modulus are described in the literature: the dilatometric method pioneered by Goldbach and Rehage¹² and later taken up by Simon and co-workers,^{13,14} the "acoustic method" first developed by McKinney *et al.*¹⁵ and later described by Knauss and co-workers,^{16,17} and the piezo-electric bulk modulus gauge (PBG) technique¹⁸ developed in our group some time ago for measuring the adiabatic bulk modulus $K_S(\omega)$. In the "dilatometric method" a liquid-filled sample chamber is connected to a capillary. The sample's volume response to an imposed step in pressure is monitored by the height of the liquid in the capillary.¹² Using a pressure gauge with a feedback mechanism makes it possible to keep the sample volume fixed and monitor the pressure change instead.^{13,14} The "dilatometric method" is a time-domain technique and quite long times are monitored ($\sim 10^2 - 10^6$ s). Thus, the measured quantity is the *isothermal* bulk modulus (or bulk creep compliance). In the "acoustic method" piezo-electric plates are used in a transmitter-receiver mode: one plate is used to generate an oscillating hydrostatic pressure change in the oil surrounding the sample causing a volumetric deformation of the sample. The other disc then detects pressure changes in response. This technique works in the frequency domain (covers roughly 10 - 1000 Hz) and measures the adiabatic bulk modulus.

Here, we present results obtained with PBG technique.¹⁸ This technique is also based on the piezo-electric effect, but in this case using the piezo-electric material as a transducer in direct contact with the sample, generating a volume oscillation and measuring the response simultaneously (more details are given in Sec. II). The PBG covers a wide dynamical window (~ 7 decades in frequency from roughly 1 mHz

to 10 kHz). The thermal diffusion length at all frequencies is much smaller than the sample dimension, which means that we measure the *adiabatic* bulk modulus, K_S .

The paper is structured as follows: After an introduction to the technique in Sec. II, we proceed to present our results in Sec. III. First, we show the raw data for the measured dynamic adiabatic bulk moduli (Sec. III A), and then analyze the data in terms of relaxation times (Sec. III B), spectral shapes (Sec. III C) – also in comparison to their shear mechanical counterparts – the relaxation strength (Sec. III D), and finally, we test a bulk modulus version of the shoving model (Sec. III E).

II. EXPERIMENTAL DETAILS

The PBG technique utilizes the coupling between the capacitance of a piezo-electric spherical shell and the stiffness of a liquid inside the shell. The bulk transducer is a spherical shell of piezo electric ceramic material polarized in the radial direction. The inner and outer surfaces of the shell are coated with silver electrodes and connected to an ac voltage generator. The potential difference between the inner and outer surface of the transducer causes the polarized shell to deform, thus inducing a bulk deformation of a liquid contained within the piezo electric shell. The motion of the shell is hindered by the stiffness of the liquid, and the measured capacitance of the shell thus depends on whether the transducer is empty and freely moving or filled. By measuring the difference between the capacitance of the empty transducer (the “reference measurement”) and the liquid-filled transducer (the “liquid measurement”), the bulk modulus of the liquid can be calculated, see Refs. 18–20 for more details.

The transducer has a small hole at the top and is equipped with a tube that functions as a liquid reservoir. Figure 1 shows a sketch of the device. When the transducer is loaded at room temperature, it is filled with liquid to the top of the tube. This ensures that the sphere is always filled with liquid, also at

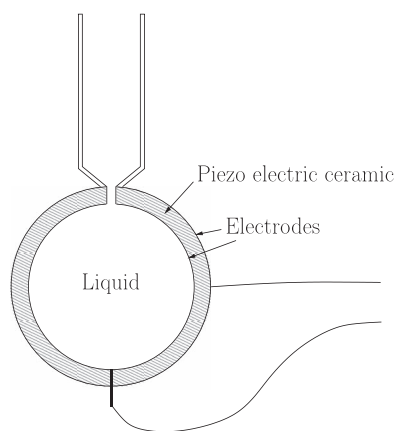


FIG. 1. Sketch of the bulk transducer (PBG).^{18,19} The device consists of a shell made of a piezo-electric ceramic material coated with silver electrodes on the inside and outside. Wires connect the two electrodes to a voltage generator. The inner diameter of the sphere is 18 mm and the thickness of the ceramics is 0.5 mm. A small hole (diameter $d = 1.9$ mm) in the shell makes it possible to fill the bulk transducer with liquid. A tube acting as a liquid reservoir is attached on top of the hole. This ensures that the sphere is always filled with liquid, even as the liquid contracts upon cooling.

lower temperatures where the liquid volume decreases due to thermal contraction. The presence of the hole limits the frequency range for measuring the bulk modulus, since the liquid is able to flow out of the sphere at low frequencies (how low depends on the viscosity of the liquid and thus on the temperature). As shown recently, it is possible however to extend the frequency range by modeling the flow through the hole and subtracting the contribution to the measured signal.^{19,20} On the high frequency side, the frequency window is limited by the mechanical resonance of the transducer, which lies between 10 and 100 kHz. Consequently, we are able to measure the dynamic bulk modulus in a wide dynamical range from roughly 10 mHz to 10 kHz.

Temperature is controlled in a closed-cycle cryostat with a temperature stability of ~ 10 mK and an absolute temperature uncertainty of less than 0.1 K. The temperature control and measuring setup is described in detail in Refs. 21 and 22. Temperature stability is crucial for the calculation of the bulk modulus, since it relies on good agreement between liquid and reference measurement. The properties of the transducer itself depends both on temperature *and* thermal history (discussed in Refs. 19 and 23), so it is essential that the experimental protocol for the two measurements is identical.

The studied liquids are trimethyl-pentaphenyl-trisiloxane (DC705), dibutyl phthalate (DBP), and 1,2-propanediol (PD). All liquids were purchased from Sigma-Aldrich. DC705 and DBP were used as acquired, PD was dried for several hours in a vacuum exicator at ambient temperature. These liquids were chosen because data from other response functions (in particular, shear modulus data) exist for comparison. In addition, they are stable and easy to handle at room temperature.

III. RESULTS

A. The raw data

Figure 2 shows real and imaginary parts of the bulk modulus for DBP, DC705, and PD. The data exhibit a transition in the real part from a low-frequency level, K_0 , corresponding to a liquid-like response, to a high frequency level, K_∞ , corresponding to a solid-like response (however, the high frequency plateau is not reached for all temperatures due to the upper limit in frequency span). This transition shows up as a peak in the imaginary part that moves down in frequency with decreasing temperature.

For all liquids, the peak height increases with decreasing temperature, corresponding to an increase in relaxation strength, ΔK . For DC705, however, the increase at the lowest temperatures is anomalously high. This is presumably an artifact of a combination of two factors in the measurement and subsequent analysis, namely, (1) a slight difference in the frequency dependence of the liquid and the reference spectrum, and (2) an imperfect filling of the transducer at the lowest temperatures: (1) The piezo-electric ceramic material of the transducer has a weak frequency dependence at low frequencies due to dispersion of permittivity of the ceramics. The data analysis relies on the premise that this frequency dependence is the same for the liquid and the reference measurement. The raw capacitance data of DC705 show a slight mismatch in the

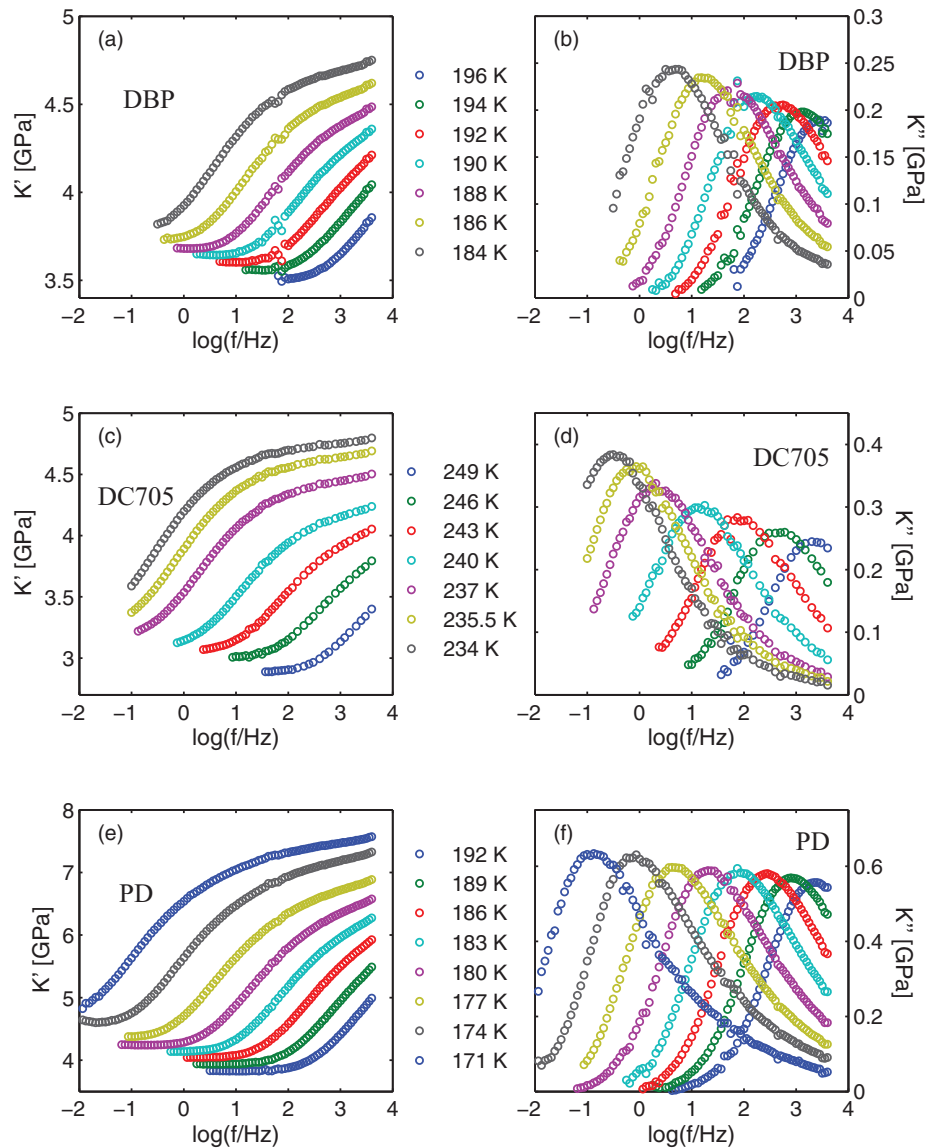


FIG. 2. Real and imaginary parts of bulk modulus for DBP (a)+(b), DC705 (c)+(d), and PD (e)+(f). At low frequencies, a (non-vanishing) liquid-like plateau is observed in the real part of the modulus; at high frequencies, a solid-like (higher) plateau is approached. For most of the temperatures, the solid-like plateau is however outside the frequency window. Both plateau values increase as the temperature is lowered. Between the two plateaus there is a transition from liquid-like to solid-like behavior, which shows up as a peak in the imaginary part. As with all dynamical quantities in a liquid close to the glass-transition temperature, the characteristic time of this transition is dramatically increased with decreasing temperature; here, changing 5 orders of magnitude with a temperature change of only 15 K (corresponding to roughly 6%) in the case of DC705.

frequency dependence, however, which results in an increasing imaginary part and a small slope on the plateaus of the real part of the bulk modulus. (2) The aforementioned flow to and from the reservoir gives rise to a resonance at low frequencies – the “Helmholtz resonance”²⁰ – which can be subtracted from the raw data to extend the frequency range of calculated bulk modulus. This subtraction should in principle result in an imaginary part that goes to zero on both sides of the loss peak, and a real part with constant high and low frequency plateaus. For DC705, the low-frequency side of the loss peak does not go to zero at the lowest temperatures even after subtracting the contribution from the Helmholtz resonance. This is sometimes seen when the liquid for some reason is not able to draw in extra liquid from the reservoir at the lowest temperatures, resulting in a cavity inside the transducer that breaks

the spherical symmetry. The accuracy of the bulk modulus for the lowest three temperatures is hence poorer than the other temperatures. We made a conservative low-frequency cutoff of the data to avoid these artifacts, but they can still influence the shape of the low-frequency flank of the alpha-relaxation peak. We do, however, believe that the high-frequency side of the peak remains unaffected by these problems and that the extracted relaxation times are correct within the overall accuracy of the data sets.

In the data, there is a slight upturn of the real part as the high frequencies are approached. This is an artifact of the inversion procedure described in the previous paragraph. It comes from the fact that the first resonance of the liquid-filled PBG is located at a slightly lower frequency compared to the empty device. Thus, the procedure that eliminates the effect

of dispersion of the ceramic at low frequencies, introduces a small artifact towards the high frequencies.

B. Relaxation times

To quantify the temperature dependence of the relaxation time for the bulk modulus, we estimated the loss-peak frequencies of the imaginary parts by fitting a second-order polynomial to the maximum nine points (which corresponds to less than half a decade in frequency) around the maximum of $\log(f)$ vs $\log(K'')$. This is usually a good measure of the time scale of the alpha relaxation. However, when the data are noisy this procedure may lead to errors and thus we also defined an integrated (or “average”) relaxation frequency as the normalized real part integrated over all frequencies,^{51,52}

$$\begin{aligned} \langle f \rangle &= \frac{1}{\pi^2 \Delta K} \int_0^\infty (K'(f) - K_\infty) df \\ &= \frac{1}{\pi^2 \Delta K} \int_{-\infty}^\infty (K'(f) - K_\infty) f d \ln f, \end{aligned} \quad (1)$$

where f is the frequency. The factor $1/\pi^2$ ensures that this integral gives $1/(2\pi\tau)$ if applied to an exponential. This expression yields slightly faster relaxation times (or higher average frequencies) than the peak frequency, because of the stretched, non-exponential relaxation, which is a hallmark feature of viscous liquids.

Figure 3(a) shows a plot of the loss-peak frequency and the average frequency as a function of temperature. As expected the peak frequencies are slightly lower than the average frequency, but otherwise the two measures of time scale are proportional. There are slightly fewer temperatures for which the average frequency could be determined. This is because the spectra at high temperatures get cut off by the experimental frequency window, thus making it impossible to do the integration reasonably, while it is still possible to determine a peak frequency. All three liquids display a non-Arrhenius behavior of bulk relaxation time, in harmony with the corresponding shear modulus data.²⁴ Unfortunately, these shear modulus measurements were not carried out in the same cryostat as the bulk modulus measurements. To compare the temperature dependence of the time scales reliably, the absolute temperature difference between cryostats was calibrated by means of dielectric measurements, resulting in adjustments up to ± 1.5 K of the temperatures.

In the relaxation map, the time scales for bulk and shear moduli are difficult to distinguish, in particular when we want to quantify whether the time scales are coupled (i.e., proportional) or possibly have different temperature dependence. The “time scale index”²⁵ (defined as the ratio of the characteristic times of the two response functions as a function of temperature) is a very sensitive measure for this. In Fig. 3(b), we compare the bulk relaxation time scale to the corresponding shear time⁵³ by calculating the “time scale index” both for the determined peak frequencies (full symbols) and the average frequencies (open symbols). There is no clear trend in the temperature dependence of the time scale index; the result depends on how the time scale is defined. For DC705, there is a lot of scatter in the peak frequency measure, while

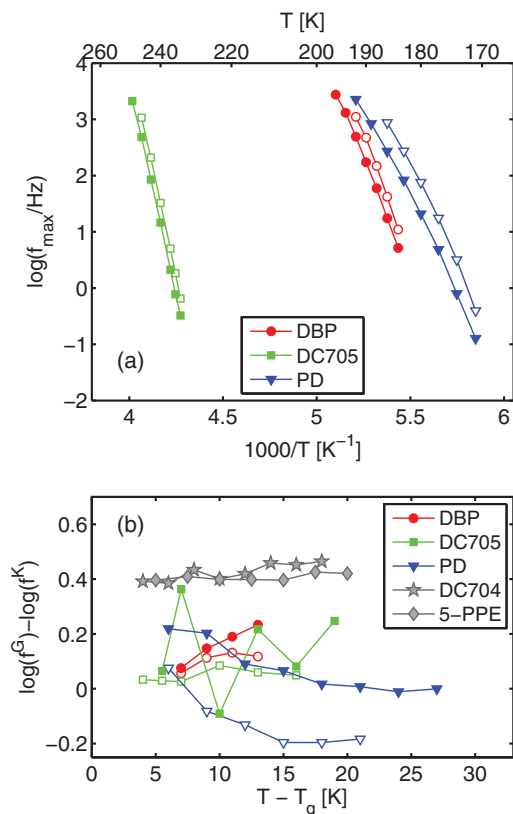


FIG. 3. Characteristic time scales of the bulk modulus relaxation. (a) Loss-peak frequencies of the bulk modulus (full symbols) and average frequency $\langle f \rangle$, see Eq. (1), (open symbols) as a function of inverse temperature for the three liquids. (b) Time scale index of bulk and shear moduli. Only four temperatures are shown for DBP, which corresponds to the overlap in temperatures between the shear and bulk modulus measurement. For comparison, previous results²⁰ for tetraphenyl-tetramethyl-trisiloxane (DC704) and 5-phenyl-4-ether (5-PPE) are shown.

the average frequencies give a nearly constant time scale index. For DBP, the overlap in temperatures of the two measurements was small so we have only four time scale index points. Here, the peak frequency measure seems to have an increasing trend with temperature while the average frequency measure is nearly constant. For PD, the time scale index is positive when the peak frequencies are used, while it is negative when we use the average frequencies.

Earlier studies of shear and bulk modulus relaxation^{6,7,26} have shown that the shear relaxation is faster than the bulk modulus relaxation and again recently this was found²⁰ to be the case for two liquids with a temperature-independent factor of around 0.4 decade (shown in Fig. 3(b) for comparison). In the present case, there is notably more noise and in contrast to Hecksher *et al.*,²⁰ the compared measurements are performed in different cryostats. The time scale index is quite sensitive to small errors both in temperature and in relaxation times,¹⁹ so although we have tried to eliminate sources of error, we have to be cautious about drawing conclusions. For PD, the decoupling seems persistent, though, while Fig. 3(b) indicates that the time scales of shear and bulk modulus for DC705 and DBP are identical within the noise of the data.

The decoupling or coupling of time scales in general for viscous liquids is a matter of debate. Often studied are the Stokes-Einstein and Debye-Stokes-Einstein relations

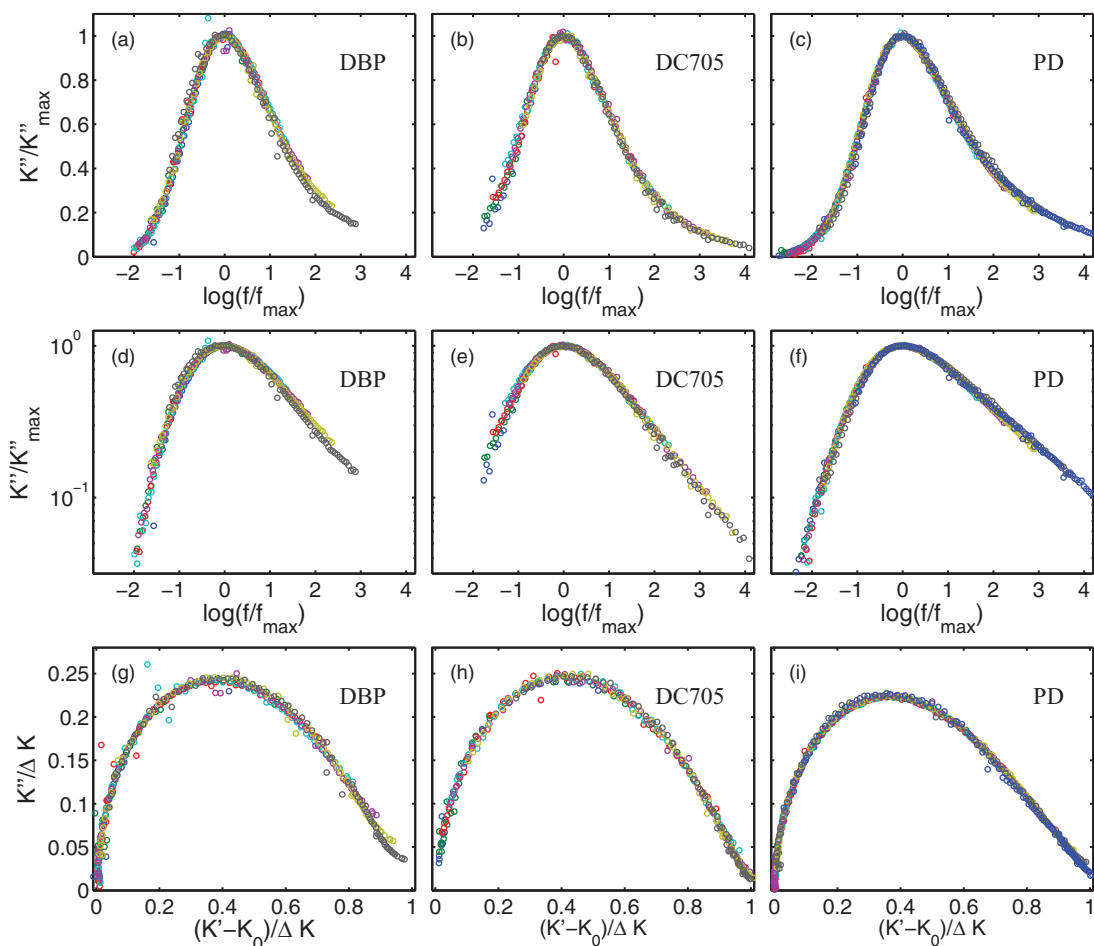


FIG. 4. Time-temperature superposition (TTS) plots of DBP, DC705, and PD. The top panels (a)–(c) show the imaginary parts of data scaled by the loss-peak value on a linear axis versus the logarithm of frequency scaled by the loss peak frequency for each temperature. The middle panels (d)–(f) show the scaled imaginary parts on a logarithmic axis as a function of scaled frequency. The bottom panels (g)–(i) show the scaled imaginary part versus the scaled real part (referred to as a “Cole-Cole plot”). Clearly, all three liquids obey TTS within the noise in both real and imaginary parts.

$D \propto T/\eta$ linking the translational or rotational diffusion D of a (large) object suspended in the liquid to the viscosity η . These quantities are often found to decouple with decreasing temperature,^{27–37} especially if the tracer molecule is comparable in size to the molecules of the matrix. Studies of time scales of different response functions – such as dielectric constant and shear modulus – on the other hand often show weak or no decoupling,^{20,25,26,38–42} but examples exist where the opposite is observed.⁴³

The lack of generality in the literature and in the present results could well be due to differences in experimental conditions (especially the temperature calibration of different cryostats, but also different samples), which once again stresses the importance of having accurate and reproducible temperature control and only comparing response functions that are measured simultaneously or at least under identical experimental conditions.

C. Spectral shapes

We proceed to examine the temperature dependence of the spectral shapes of the bulk modulus data, in particular if time-temperature superposition (TTS) is obeyed. TTS refers to the notion of a temperature-independent spectral shape of

the alpha relaxation that simply shifts on the time/frequency axis as temperature is changed. Thus, TTS is obeyed whenever a collapse of data is obtained by scaling the loss by the loss peak height and the frequency by the loss-peak frequency.

Figure 4 shows TTS plots of the three liquids. The top two panels show the standard plot, i.e., loss modulus as a function of frequency scaled to the values where the curve has its maximum. We show this plot on both a linear (top panel) and a logarithmic (middle panel) axis. The bottom panel shows a so-called Cole-Cole plot. This is a parameterized plot displaying the imaginary part as a function of the real part both scaled by the overall relaxation strength $\Delta K = K_\infty - K_0$ (see Sec. III D below for details on how the scaling parameters were determined). This is a convenient way of showing both the real and imaginary parts in one plot scaled by the same factor. The Cole-Cole representation of the data is also quite sensitive to deviations from TTS.

The bulk modulus data show a nice collapse in both representations and we thus conclude that TTS is obeyed for all the liquids within the noise of the data, except for a very small deviation of the high-frequency side of the loss peak for DBP. This deviation could be due to a secondary process at higher frequencies, which would be in agreement with both dielectric data showing a low-intensity beta process around

10^6 Hz⁴⁴ and shear data,²⁴ where the onset of a beta process is seen in the same temperature interval. The frequency window of the bulk modulus data does not allow a definite identification of a beta process for the measured temperatures. The temperature window could be extended slightly corresponding to a change in the alpha loss-peak frequency of roughly two decades, which would reveal if the observed deviation evolves into a beta feature. The absence of a secondary process for DC705 is consistent with both shear and dielectric measurements, while the same is only partly true for PD. For this liquid, shear measurements show TTS, while dielectric measurements exhibit a wing at high frequencies.⁴⁵

In Fig. 5(a), we show a common TTS plot of the bulk modulus spectra of all three liquids with asymptotic low- and high-frequency power laws indicated by dashed lines. All liquids display an approximate low-frequency Maxwell model behavior, i.e., $K'' \propto f$, as expected for a terminal pure viscous behavior. For DBP, a slightly steeper slope is seen; this is most likely a measurement error arising from imperfect matching of liquid and reference measurement. At high frequencies, DBP and DC705 have similar shapes with an asymptotic power law of slope -0.4 , while PD has a smaller slope of about -0.25 and thus a much broader spectrum. Consequently, we do not in general find a correlation between TTS and a high-frequency power law of -0.5 (as found in dielectrics in Refs. 45 and 46) for the bulk modulus spectra.

Figures 5(b)–5(d) show the TTS plots of the bulk spectra for each of the three liquids together with their corresponding shear modulus spectra. Shear modulus measurements²⁴ indicate the existence of a mechanical beta process for DBP (although the peak of this relaxation was outside the frequency interval of the measurements). When comparing to the bulk modulus spectra, it is possible that the high-frequency deviation from a pure power law is a beta process appearing in the bulk modulus, as well. Bulk and shear modulus spectra are very similar within the noise and measurement errors for DC705 and DBP. For PD, there is near perfect collapse at low frequencies while the high-frequency power laws are significantly different, the bulk modulus having a much broader spectrum.

D. Relaxation strength

In Fig. 6(a), the high- and low-frequency levels of the bulk modulus are shown as functions of temperature relative to T_g . T_g was defined as the temperature at which the loss-peak frequency is 1 mHz found by extrapolating the loss peaks in Fig. 3 fitted to a VFT-expression. The plateau values are not always within the accessible frequency window for all temperatures, and thus we determined the high- and low-frequency levels of the bulk modulus from fitting to the extended Maxwell model,^{18,47,48}

$$K = K_0 + \frac{K_\infty - K_0}{1 + \frac{1}{i\omega\tau} + q(\frac{1}{i\omega\tau})^\alpha}. \quad (2)$$

Here, K_0 and K_∞ are the low- and high-frequency plateau levels, τ is the (alpha) relaxation time, and q and α are fitting

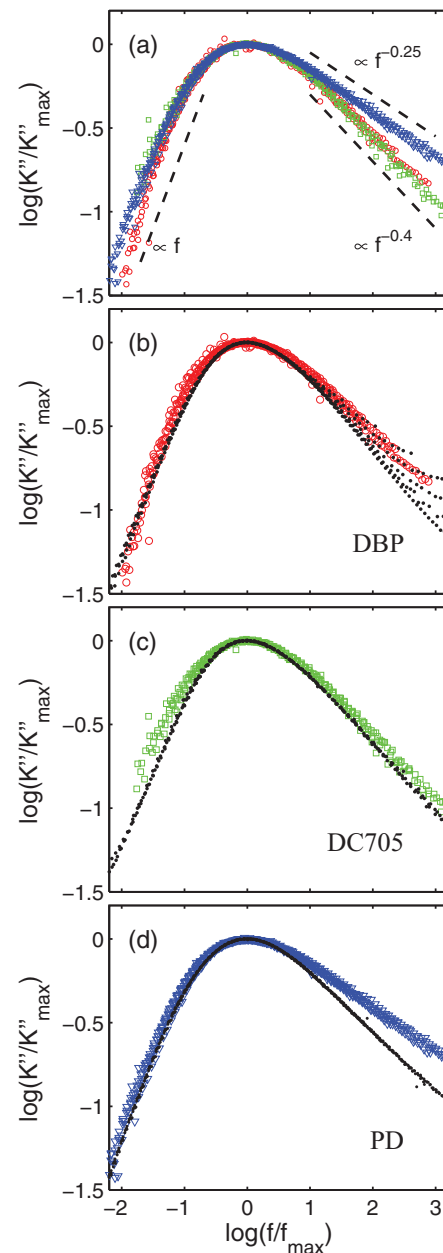


FIG. 5. TTS plots comparing bulk modulus data for the three liquids (a) and comparing to shear modulus data (b)–(d) for each of the liquids respectively. (a) All three liquids display a common low frequency “Maxwell model” behavior (indicated by a dotted line showing $K'' \propto f$). DBP and DC705 have very similar shapes for the entire spectrum, while the high frequency side of the PD spectrum displays a power law behavior with a smaller exponent. (b)–(d) Bulk (large symbols) and shear (black dots) modulus spectra are very similar for DBP and DC705, except for a slightly broader low frequency side for DC705 (which could be due to measurement errors, see text for details) and a less evident secondary relaxation in DBP at high frequencies. For PD, on the other hand, there is excellent overlap on the low-frequency side of the peak, while there is a significant difference in the high-frequency asymptotic power laws; the bulk modulus having a smaller slope than the shear modulus.

parameters expressing the peak width and the high frequency slope of the loss peak, respectively.

To limit the number of parameters in the fit and since all liquids obey TTS within the noise, we have chosen to fit the data for each liquid with a temperature independent set of the shape parameters q and α . The best values of these two

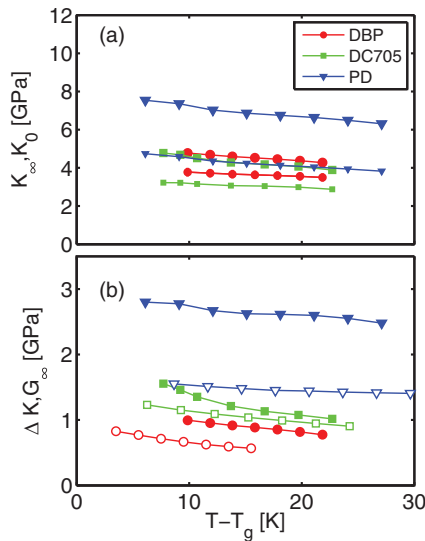


FIG. 6. Plateau levels and relaxation strength for bulk and shear modulus. (a) The fitted (see Eq. (2)) K_∞ (large symbols) and K_0 (small symbols) levels for DBP (red circles), DC704 (green squares), and DBP (blue triangles). (b) Comparison of the bulk modulus relaxation strength $\Delta K = K_\infty - K_0$ (closed symbols) with $G_\infty (= \Delta G)$ (open symbols). Evidently, the bulk relaxation strength is greater than the shear.

parameters were found by fitting the frequency spectrum of the temperature with the most data points on both sides of the loss peak to the expression in Eq. (2) with all parameters varying freely. For DBP that temperature is $T = 186$ K, for DC705 $T = 243$ K, and $T = 177$ K for PD. The rest of the temperatures for each liquid was then fitted with q and α fixed determining K_0 and K_∞ values for each temperature.

In Fig. 6(b), the relaxation strength ($\Delta K = K_\infty - K_0$) is compared to the high-frequency values of the shear modulus of Ref. 24. DBP and DC705 have comparable magnitudes of K_0 and K_∞ and relaxation strength ΔK , whereas PD has both slightly higher plateau values and a higher relaxation strength. For all three liquids, the bulk relaxation strength is larger than what is found in the shear modulus data.

E. Comparing to the prediction of the bulk modulus version of the shoving model

Finally, we test the “bulk modulus version” of the shoving model⁴⁹ for the temperature dependence of the relaxation time of viscous liquids. The shoving model is based on the assumption that the relaxation proceeds as a series of flow events. Due to anharmonicity it is energetically costly for molecules to rearrange at constant volume and a local volume increase will facilitate such a rearrangement. Flow events in themselves are fast, and the key assumptions of the shoving model are that the surrounding liquid is solid on the time scale of a flow event and that the activation energy is mainly elastic energy of the surroundings. A local volume increase induces a shear deformation of the surroundings,⁵⁰ and the activation energy is hence described by the shear modulus^{5,49}

$$\tau(T) = \tau_0 \exp \left\{ \frac{V_c G_\infty(T)}{k_B T} \right\}. \quad (3)$$

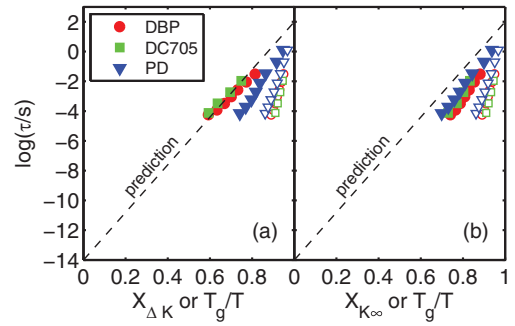


FIG. 7. Test of a “bulk modulus version” of the shoving model (Eq. (3)) substituting G_∞ by (a) the bulk modulus relaxation strength, ΔK and (b) the high-frequency level of the bulk modulus, K_∞ . Open symbols represent a standard fragility plot, i.e., the relaxation time is plotted against inverse temperature scaled by T_g . The full symbols are plotted against the X parameter (see text) and are predicted to follow the indicated dashed line (see Eq. (4)). In the first version (a), DC705 and DBP follow the prediction while PD does not, whereas in the second version (b) all three liquids fail, although PD is doing slightly better than in the first case.

Thus, the logarithm of the relaxation time is a linear function of $G_\infty(T)/T$ assuming the characteristic volume V_c is temperature independent. Under this assumption, V_c can be scaled out by constructing a parameter $X = \frac{G_\infty(T)/T}{G_\infty(T_g)/T_g}$ running from 0 to 1. In the “shoving plot,” $\log \tau$ is plotted as a function of X , and data should follow a straight line going from the pre-factor τ_0 to $\tau(T_g)$ defined to be 100 s. Taking the pre-factor to be $\tau_0 = 10^{-14}$ s, the prediction of the shoving model can be rewritten as

$$\log(\tau(T)) = 16X - 14. \quad (4)$$

If $\Delta K(T) \propto G_\infty(T)$ (as indicated in Fig. 6(b)), we can substitute the bulk modulus relaxation strength into this expression. It is also interesting to see whether $G_\infty(T)$ can be replaced by $K_\infty(T)$ in the model. Again, if $K_\infty(T) \propto G_\infty(T)$, they can be swapped in the shoving plot and give the same result. Both $\Delta K(T) \propto G_\infty(T)$ and $K_\infty(T) \propto G_\infty(T)$ need not be true at the same time, but it is interesting to see which (if any) is valid.

In Fig. 7(a), we show relaxation times plotted as a function of $X_{\Delta K} = (\Delta K(T)/T)/(\Delta K(T_g)/T_g)$ and in Fig. 7(b) as a function of $X_{K_\infty} = (K_\infty(T)/T)/(K_\infty(T_g)/T_g)$. For DC705, the three lowest temperatures were not included in the analysis because of an unphysical increase in relaxation strength discussed in the beginning of Sec. III A which is reflected in Fig. 6(b).

The shoving model with G_∞ replaced by ΔK describes DBP and DC705 well, while PD does not follow the predicted line. In the case of PD, replacing G_∞ by K_∞ gives a slightly better result. Maggi *et al.*²⁴ found the shoving model (with the measured $G_\infty(T)$) to give a good description of DC705 and PD (DBP was not tested since DBP was not found to obey TTS in the shear modulus spectra), but one must keep in mind that the remeasured PD shear spectra did not reproduce the previously published data, which we speculate to be due to different water content.

IV. SUMMARY

We have presented measurements of the adiabatic bulk modulus for three glass-forming liquids and compared them to measurements of the shear modulus for the same liquids. The bulk modulus spectra for all three liquids obey TTS within the noise. DBP and DC705 show very similar behavior with respect to spectral shapes, relaxation strength, high- and low-frequency levels (K_∞ and K_0), and in their similarity with corresponding shear modulus spectra. PD differs by having a higher modulus, higher relaxation strength, and significant difference between bulk and shear modulus spectra. The bulk modulus was found to relax on roughly the same time scale as the shear modulus for all three liquids, and it was not possible to draw any clear conclusion about the decoupling of shear and bulk relaxation. DC705 and DBP follow a formal reformulation of the shoving model with G_∞ replaced by the bulk modulus relaxation strength ΔK , while replacing G_∞ with K_∞ gives a poor result for all three liquids. Thus, the two van der Waal's bonded liquids (DBP and DC705) display a "simpler" behavior and differ quantitatively and qualitatively from the hydrogen-bonded PD in the spectral features studied here.

ACKNOWLEDGMENTS

Kristine Niss wishes to acknowledge The Danish Council for Independent Research for supporting this work. The centre for viscous liquid dynamics "Glass and Time" is sponsored by the Danish National Research Foundation (Grant No. DNRF61).

- ¹M. D. Ediger, C. A. Angell, and S. R. Nagel, *J. Chem. Phys.* **100**, 13200 (1996).
- ²P. G. Debenedetti and F. H. Stillinger, *Nature (London)* **410**, 259 (2001).
- ³A. Cavagna, *Phys. Rep.* **476**, 51 (2009).
- ⁴G. Harrison, *The Dynamic Properties of Supercooled Liquids* (Academic Press, 1976).
- ⁵J. C. Dyre, *Rev. Mod. Phys.* **78**, 953 (2006).
- ⁶E. Morita, R. Kono, and H. Yoshizak, *Jap. J. Appl. Phys.* **7**, 451 (1968).
- ⁷A. R. Dexter and A. J. Matheson, *J. Chem. Phys.* **54**, 3463 (1971).
- ⁸V. A. Solov'yev, Y. S. Manucharov, and I. Alig, *Acta Polym.* **40**, 513 (1989).
- ⁹I. Alig, F. Stieber, A. D. Bakhranov, Y. S. Manucharov, S. A. Manucharova, and V. A. Solov'yev, *Polymer* **31**, 877 (1990).
- ¹⁰L. D. Landau and E. M. Lifshitz, *Theory of Elasticity* (Elsevier, 1986).
- ¹¹N. W. Tschoegl and W. G. Knauss, *Mech. Time-Dep. Mat.* **6**, 3 (2002).
- ¹²G. Goldbach and G. Rehage, *Rheol. Acta* **6**, 30 (1967).
- ¹³Y. Meng and S. L. Simon, *J. Polym. Sci. Part B: Polym. Phys.* **45**, 3375 (2007).
- ¹⁴Y. Meng, P. Bernazzani, P. A. O'Connell, G. B. McKenna, and S. L. Simon, *Rev. Sci. Instrum.* **80**, 053903 (2009).
- ¹⁵J. E. McKinney, S. Edelman, and R. S. Marvin, *J. Appl. Phys.* **27**, 425 (1956).
- ¹⁶T. H. Deng and W. G. Knauss, *Mech. Time-Dep. Mat.* **1**, 33 (1997).
- ¹⁷S. B. Sane and W. G. Knauss, *Mech. Time-Dep. Mat.* **5**, 293 (2001).
- ¹⁸T. Christensen and N. B. Olsen, *Phys. Rev. B* **49**, 15396 (1994).
- ¹⁹T. Hecksher, Ph.D. thesis, Roskilde University, 2010.
- ²⁰T. Hecksher, N. B. Olsen, K. A. Nelson, J. C. Dyre, and T. Christensen, *J. Chem. Phys.* **138**, 12A543 (2013).
- ²¹B. Igarashi, T. Christensen, E. H. Larsen, N. B. Olsen, I. H. Pedersen, T. Rasmussen, and J. C. Dyre, *Rev. Sci. Instrum.* **79**, 045105 (2008).
- ²²B. Igarashi, T. Christensen, E. H. Larsen, N. B. Olsen, I. H. Pedersen, T. Rasmussen, and J. C. Dyre, *Rev. Sci. Instrum.* **79**, 045106 (2008).
- ²³T. Christensen and N. B. Olsen, *Rev. Sci. Instrum.* **66**, 5019 (1995).
- ²⁴C. Maggi, B. Jakobsen, T. Christensen, N. B. Olsen, and J. C. Dyre, *J. Phys. Chem. B* **112**, 16320 (2008).
- ²⁵B. Jakobsen, T. Hecksher, T. Christensen, N. B. Olsen, J. C. Dyre, and K. Niss, *J. Chem. Phys.* **136**, 081102 (2012).
- ²⁶T. Christensen and N. B. Olsen, *J. Non-Cryst. Solids* **172–174**, 362 (1994).
- ²⁷E. Rössler, *Phys. Rev. Lett.* **65**, 1595 (1990).
- ²⁸F. Fujara, B. Geil, H. Sillescu, and G. Fleischer, *Z. Phys. B* **88**, 195 (1992).
- ²⁹E. Rössler and P. Eiermann, *J. Chem. Phys.* **100**, 5237 (1994).
- ³⁰J. C. Hooker and J. M. Torkelson, *Macromolecules* **28**, 7683 (1995).
- ³¹M. T. Cicerone and M. D. Ediger, *J. Chem. Phys.* **104**, 7210 (1996).
- ³²I. Chang and H. Sillescu, *J. Phys. Chem. B* **101**, 8794 (1997).
- ³³A. Voronel, E. Veliyulin, V. S. Machavariani, A. Kisliuk, and D. Quitmann, *Phys. Rev. Lett.* **80**, 2630 (1998).
- ³⁴S. Corezzi, E. Campani, P. A. Rolla, S. Capaccioli, and D. Fioretto, *J. Chem. Phys.* **111**, 9343 (1999).
- ³⁵L.-M. Wang, V. Velikov, and C. A. Angell, *J. Chem. Phys.* **117**, 10184 (2002).
- ³⁶E. L. Gjersing, S. Sen, P. Yu, and B. G. Aitken, *Phys. Rev. E* **76**, 214202 (2007).
- ³⁷J. R. Rajian and E. L. Quitevis, *J. Chem. Phys.* **126**, 224506 (2007).
- ³⁸R. Zorn, F. I. Mopsik, G. B. McKenna, L. Willner, and D. Richter, *J. Chem. Phys.* **107**, 3645 (1997).
- ³⁹R. D. Deegan, R. L. Leheny, N. Menon, S. R. Nagel, and D. C. Venerus, *J. Phys. Chem. B* **103**, 4066 (1999).
- ⁴⁰W. Suchanski, S. Jurga, T. Pakula, M. Paluch, and J. Ziolo, *J. Phys.: Condens. Matter* **12**, 9551 (2000).
- ⁴¹K. Schröter and E. Donth, *J. Non-Cryst. Solids* **307–310**, 270 (2002).
- ⁴²C. Dreyfus, S. Murugavel, R. Gupta, M. Massot, R. M. Pick, and H. Z. Cummins, *Philos. Mag. B* **82**, 263 (2002).
- ⁴³D. H. Torchinsky, J. A. Johnson, and K. A. Nelson, *J. Chem. Phys.* **136**, 174509 (2012).
- ⁴⁴P. K. Dixon, L. Wu, S. R. Nagel, B. D. Williams, and J. P. Carini, *Phys. Rev. Lett.* **65**, 1108 (1990).
- ⁴⁵A. I. Nielsen, B. Jakobsen, K. Niss, N. B. Olsen, R. Richert, and J. C. Dyre, *J. Chem. Phys.* **130**, 154508 (2009).
- ⁴⁶N. B. Olsen, T. Christensen, and J. C. Dyre, *Phys. Rev. Lett.* **86**, 1271 (2001).
- ⁴⁷N. Saglanmak, A. I. Nielsen, N. B. Olsen, J. C. Dyre, and K. Niss, *J. Chem. Phys.* **132**, 024503 (2010).
- ⁴⁸B. Jakobsen, K. Niss, C. Maggi, N. B. Olsen, T. Christensen, and J. C. Dyre, *J. Non-Cryst. Solids* **357**, 267 (2011).
- ⁴⁹J. C. Dyre, N. B. Olsen, and T. Christensen, *Phys. Rev. B* **53**, 2171 (1996).
- ⁵⁰J. C. Dyre and N. B. Olsen, *Phys. Rev. E* **69**, 042501 (2004).
- ⁵¹R. Zorn, *J. Chem. Phys.* **116**, 3204 (2002).
- ⁵²This integral is well-defined in contrast to the integral over the imaginary part which diverges. There are different ways of handling this. Zorn⁵¹ suggests to make an average logarithmic frequency, i.e., integrate over $\ln f$ with the normalized imaginary part as a weight.
- ⁵³Shear spectra for PD were remeasured since it is a hygroscopic substance. The new spectra were very different with respect to time scales, shapes, and absolute values. The new shear modulus data were measured on the same bottle (a dried sample) as the bulk modulus and within weeks of each other so we believe that the two sets of data are really on the same liquid. All data are available at the "Glass and Time" data repository at <http://glass.ruc.dk/data>.